Simultaneous velocity and pressure measurements using luminescent microspheres

Fletcher Kimura,[1] Jesse McCann,[1] Gamal E. Khalil,[1] Dana Dabiri,[2] Younan Xia,[3] and James B. Callis[1]
[1]*Department of Chemistry, University of Washington, Seattle, Washington 98195, USA*
[2]*Department of Aeronautics and Astronautics, University of Washington, Seattle, Washington 98195, USA*
[3]*Department of Biomedical Engineering, Washington University, St. Louis, Missouri 63130, USA*

(Received 22 December 2009; accepted 13 April 2010; published online 4 June 2010)

Using the technique of modified rapid lifetime determination, pressure-sensitive microspheres, known as PrSBeads, were used to make quantitative oxygen measurements over two-dimensional areas within gaseous flows. Aerosolized PrSBeads in carrier gases of varying oxygen concentrations demonstrated point measurement precisions on the order of 0.1%–1%. A charge-coupled device featuring a double image frame (DIF) feature was used to make spatially resolved pressure measurements within gas phase flows. Errors on the order of 0.5 atm for one standard deviation were demonstrated when 2×2 pixel binning (162×128 pixel overall resolution) was used, but improved to 0.003–0.005 atm with the use of 32×32 pixel binning (10×8 pixel overall resolution). Experiments demonstrate the ability to resolve the oxygen concentration differences between a N_2 jet and the surrounding ambient air environment and the ability to measure instantaneous air pressure changes within a square syringe as the plunger is moved in and out. In addition, instantaneous velocity measurements of the airborne PrSBeads in a square syringe were achieved using digital particle image velocimetry at frame rates of 6.4 Hz, thus validating PrSBeads as a tool to simultaneously measure the velocity and pressure within an aerodynamic flow.
 [doi:10.1063/1.3422324]

I. INTRODUCTION

In this paper, the pressure and velocity within aerodynamic flows are determined optically through the use of aerosolized pressure sensitive particles known as PrSBeads. PrSBeads are highly uniform, polystyrene microspheres, 2.5 μm in diameter, that are doped with an oxygen-sensitive organometallic luminophor, platinum octaethylporphyrin (PtOEP). This luminophor, when subjected to a modulated excitation source, such as that of a pulsed laser at 532 nm, will enter a singlet excited state, $^1S_1$. From here, the luminophor may lose energy either through fluorescence or nonradiative decay, or undergo an intersystem crossing process and enter a triplet excited state $^3T_1$. For PtOEP, $^3T_1$ yields are very high ($\approx$100%) due to strong spin-orbit coupling induced by the presence of the heavy platinum atom.[1] The triplet excited state then decays by either emitting photons, transferring the energy to molecular oxygen, or through a nonradiatively as heat. Since the emission of photons involves an electron spin flip to relax to the singlet ground state, ^1S_o, the process is differentiated from fluorescence where no spin flip is necessary. Here, the emission is known as phosphorescence, and can occur over timescales on the order of milliseconds to seconds.[2] The phosphorescence ideally follows an exponential decay[3] of the form

$$I = I_o e^{(-t/\tau)} + D_o, \tag{1}$$

where I_o represents the initial intensity of luminophor upon excitation, t is time, τ is the lifetime (duration) of the phosphorescence, and D_o is the background signal. Lifetimes for this system range between 17 μs at 21% oxygen (1 atm) and 92 μs at 0% oxygen.

However, competing with phosphorescence is collision quenching by molecular oxygen. The two processes are inversely proportional—lower concentrations of surrounding oxygen leads to more phosphorescence and longer phosphorescence lifetimes, and vice versa. The lifetime can be quantitatively determined by directly relating it to the oxygen concentration in the polystyrene microsphere that surrounds the luminophor.[4] Henry's Law states that this concentration is in equilibrium with the partial pressure of oxygen surrounding the microsphere.[1] Therefore, since the partial pressure of oxygen is directly proportional to the overall atmospheric pressure, lifetime determination can provide a direct measure of the air pressure in the environment immediately surrounding the microsphere in three-dimensional space.

The lifetimes of PrSBeads can be measured using photodiodes or photomultiplier tubes designed to collect emission intensity in a time dependent manner. However, these detectors cannot provide spatially resolved lifetime data over two-dimensional areas. Fortunately it is possible to use a charge-coupled device (CCD) to obtain spatial distributions of lifetimes.[5–7] Lifetime can be determined by digitizing the luminescence decay curve following pulse excitation and data are then subjected to an appropriate fitting routines.[8] A simplified method for measuring lifetime was first proposed by Waite *et al.*,[9] known as rapid lifetime determination (RLD). In this technique, the luminescence decay is integrated over two periods of time and the lifetime is calculated

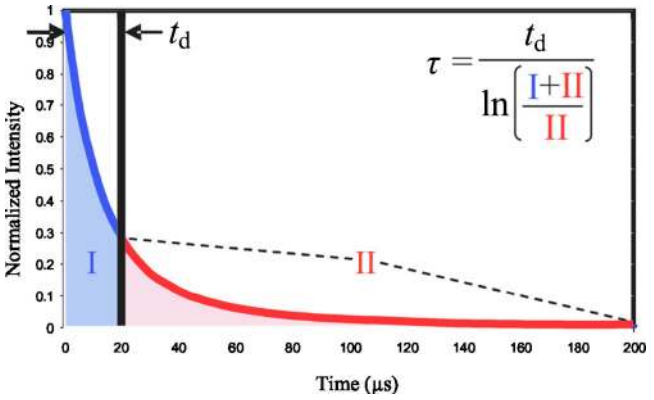

FIG. 1. (Color online) The modRLD method for the calculation of lifetime from time domain imaging. Here, the value of t_d=20 μs. I and II represent the integrated areas under their respective portions of the decay curve.

using the ratio of the integrals. In series of studies the Demas research group further developed an optimized RLD method that produced robust algorithm and improved precision performance.[10] The RLD technique was successfully used by Ni and Melton[11] to quantitatively determine the fuel equivalence for gaseous methane jets.

For this work the RLD will be used for a quantitative two-dimensional lifetime measurements by monitoring the luminescence of the PrSBeads following pulsed excitation. Using a modified version of this technique,[5] (later referred to in this paper as the modified rapid lifetime determination or modRLD method), it can be shown that by dividing the phosphorescent exponential decay curve into two regions (I and II) split at time t_d and integrating each region, a lifetime value can be calculated using

$$\tau = \frac{t_d}{\ln\left(\frac{I+II}{II}\right)}, \tag{2}$$

where I and II are the integrated areas of regions I and II, respectively (Fig. 1).

Specially designed CCD's have the ability to obtain two images in rapid succession, separated by times as small as 200 ns. Known as the double image feature (DIF),[12] it allows the user to set the exposure time of both windows, which can be as short as 1 μs. As each image effectively integrates the emission intensity of their respective portions of the phosphorescence decay curve, it is possible to calculate the spatially resolved lifetime distributions, and thus the pressure distribution, over the test area.

The appeal of this technique is the elimination of a reference or "wind-off" measurement that is inherent in intensity-based pressure measurement methods. Intensity-based measurements are sensitive to variations in paint thickness, luminophor concentration, and illumination intensity, and require a reference image to correct for these aberrations. However, proper alignment of the reference and test images is a nontrivial task, as the test subject often moves between the time the reference image is taken and actual test images are acquired. As a result, time intensive image registration methods are often required.[13]

Theoretically, since the modRLD technique acquires two images in a very short time frame that is on the order of microseconds, model movement can be considered negligible. As a result, modRLD can also be used in situations where the test subject is continually moving and a reference image would be impossible to acquire. A good example of this was demonstrated by Dale *et al.*,[6] where lifetime measurements of pressure sensitive paint (PSP) coated on the surface of a missile were made as it was dropped from a model airplane.

Therefore, this technique was considered advantageous for obtaining lifetime measurements of airborne PrSBeads. As airborne PrSBeads were expected to be continuously moving, a reference image that would correct for particle density differences from image to image would be impossible to obtain. The modRLD eliminates the need for such a reference image. However, the obstacle facing this project was the ability to obtain enough signal-to-noise from individual PrSBeads to make quantitative pressure measurements. It was found that attempting to detect the emission from a single, 2.5 μm diameter PrSBead in a macrofield of view was nearly impossible with the available hardware.

A solution to this problem was to image the collective phosphorescence of a large number of PrSBeads in a given region. Ideally, the airborne PrSBead particle density would be high enough so that all of the pixels of the imaging CCD would be filled with phosphorescent emission, much in the way laser-induced fluorescence is used to monitor molecular mixing in gaseous flows.[14] This way, it was no longer necessary to resolve and detect the phosphorescence of a single PrSBead. Instead, pixel intensity would represent the phosphorescence of many PrSBeads. However, care must be taken so that the particle density is not high enough to alter the flow and particles must be imaged such that they are individually identifiable in order for particle image velocimetry (PIV) algorithms to be applicable.[15,16]

Here, work is presented that demonstrates the feasibility of this approach, where quantitative pressure measurements within gas phase flows can be made with airborne PrSBeads. Previously, Abe *et al.*[17] have attempted to perform similar measurements using silicon dioxide microspheres containing a ruthenium-based oxygen-sensitive complex $\{[Ru(bpy)_3]Cl_2\}$, but with limited success. The authors demonstrated the feasibility of the concept by seeding a N_2 jet with these microspheres and measuring the oxygen concentration of the gas as it emptied into an ambient air chamber. While promising, the researchers were only able to measure oxygen concentrations between 0 and 0.5%, where their signal-to-noise was greatest. Additionally, while the researchers suggested that these microspheres could be used to obtain simultaneous velocimetry measurements, none were presented. In this paper, it will be shown that PrSBeads can be used to obtain quantitative pressure measurements over a range of 1 atm. Additionally, it will be shown that simultaneous velocity data can be made using PIV from the images of airborne PrSBead phosphorescent emission. Therefore, for the first time, simultaneous pressure and velocity distributions over two-dimensional areas within gas phase flows will be presented.

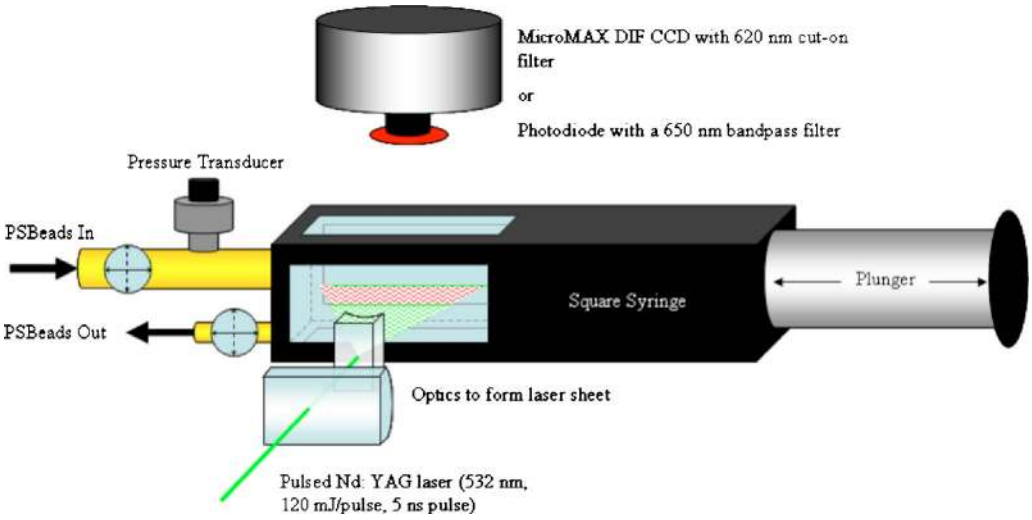

FIG. 2. (Color online) Schematic of square syringe.

II. EXPERIMENTAL PROCEDURE

Square Syringe. The primary test apparatus used in this experiment is a custom-made square-walled syringe (Fig. 2). The body of the square syringe was milled from a rectangular block of aluminum, 13.97 cm long, 3.81 cm wide, and 3.81 cm tall. A cylindrical cavity, 2.5 cm in diameter, extends the length of the block and is designed to fit the plunger of a standard 60 ml disposable syringe. A 1.9×4.4 cm^2 rectangular opening was cut into each wall of the block, 1 cm from the end. Standard glass microscope slides were adhered over these openings using UV-curable glue, thus enclosing an optically accessible volume of approximately 48.4 cm^3. All optical measurements took place within this volume. An end cap made from a two-gauge steel plate was screwed to the end of the square syringe and featured an 18 N.P.T. tapered hole, 3/8 in. (0.9525 cm) in diameter, slightly offset from the center of the plate. The PrSBeads are injected into the syringe through this opening and into the optically accessible volume. The end cap has a second, smaller opening fitted with a manually operated screw valve to allow for easy venting of the system.

The threaded opening connects the syringe to a series of tubes fitted with a manually operated lever valve and an Omega PX236 series pressure transducer (Omega Engineering, Inc., Stamford, CT). The syringe can therefore be sealed and the pressure within it continuously monitored as the plunger of the syringe is moved in and out. The Omega pressure transducer features a solid state, piezoresistive gage element designed to provide absolute pressures within $\pm 0.25\%$ of its full scale and with a response time of <1 ms. The output signal of this pressure transducer is conditioned with an in-house built preamplifier before being passed to a National Instruments data acquisition board (NI-DAQ, PCI-6110, National Instruments, Austin, TX) and processed using a virtual instrument constructed with LABVIEW. The pressure transducer is calibrated at two points (vacuum and atmospheric pressure) at the beginning of each series of experiments. A vacuum within the syringe is produced by closing the smaller vent valve and connecting the syringe to a vacuum pump. Local atmospheric pressure is verified with a mercury barometer.

The syringe volume at four different plunger locations was calibrated by submerging the entire syringe apparatus into a tank of water, then emptying it into a graduated cylinder. This procedure was repeated three times and average volumes for each of the four plunger depths were determined.

Syringe Pump. The square syringe is clamped to an in-house constructed syringe pump, which in turn is fastened securely to a three-way, *x*-*y*-*z* stage. This facilitates centering of the square syringe chamber cavity in the field of view of the CCD and the laser sheet. The syringe pump is powered by a stepper motor connected to the digital input/output port of the NI-DAQ board that provides digital control of the syringe pump, and dictates its speed and direction.

Figure 3 shows the pressure, as measured by the pressure transducer, within the sealed syringe with respect to the reciprocal of its volume $(1/V)$ as the plunger is moved in and out. The linear relationship is a condition predicted by Boyle's Law for an isothermal system[18]

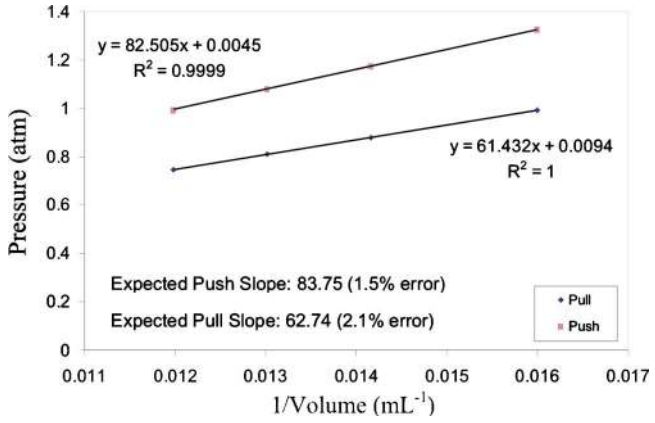

FIG. 3. (Color online) Plots of the pressure measured within the square syringe with respect to the reciprocal of its volume. The linear relationship when the plunger is pushed in and pulled out shows good agreement with theory.

$$P = nRT\left(\frac{1}{V}\right). \tag{3}$$

Assuming ideality, a linear fit of the data is expected to yield a slope equal to the value nRT, where n is the moles of gas contained in the syringe, R is the universal gas constant (0.0821 l atm mol^{-1} K^{-1}), and T is the temperature of the gas, in Kelvin. In this case, slope values of 62.7 ml atm and 83.8 ml atm are expected for the plunger moving out and in at 295 K, respectively. The different slopes are the result of different plunger starting points and thus different initial moles of gas (n). In addition, the y-intercept, where the volume of the syringe is theoretically infinity, is expected to be 0 atm. A linear least-squares fit of the data yields slopes of 61.4 and 82.5 ml atm and y-intercepts of 0.0094 and 0.0045 atm, showing good agreement with ideal gas behavior. Deviations from theory can be largely attributed to the uncertainty associated with the volume of the syringe. The ability of the syringe to hold pressure was tested by closing all valves and then increasing or decreasing the pressure within the syringe chamber with the plunger. Once at the desired position the plunger was stopped, and the pressure within the syringe chamber was monitored for 45 s. It was found that the pressure loss rates over this time period did not exceed 1.2%. Pressure losses were largest for the highest and lowest pressures being held by the syringe.

Excitation and Detection Sources. The basic optical arrangement used in these experiments is shown in Fig. 2. The primary excitation source for the airborne PrSBeads is a pulsed, 532 nm neodymium-doped yttrium aluminium garnet (Nd:YAG) laser (New Wave Research, Fremont, CA). The laser features short, 5.5 ns pulses with a maximum output energy of 120 mJ/pulse and a variable repetition rate. As a result, this laser is ideal for both PIV and lifetime measurements. The repetition rate for these experiments is 6.4 Hz, and is limited by the image acquisition rate of the CCD. The laser is aligned perpendicularly to the main axis of the syringe so the excitation beam passes through the side windows. Cylindrical lenses are used to form a laser sheet that excites a two-dimensional area ($\sim$7.6 cm^2) of airborne PrSBeads.

Time-dependent intensity measurements are made using an in-house built photodiode and preamplifier module with a measured time constant of 2 μs. The photodiode is placed directly above the top window of the syringe, normal to the incoming laser beam/sheet. When improved signal-to-noise is required, collection and focusing lenses are placed in front of the photodiode. A 650 nm bandpass filter (20 nm full-width, half-maximum) is attached to the front of the diode, along with a variable number of neutral density filters to prevent saturation. Data from the photodiode are collected by the NI-DAQ, 2500 samples per laser pulse, at a rate of 2.5 MHz.

PIV and lifetime images are acquired using a Princeton Instruments MicroMAX charge-coupled device (CCD) camera operated by WINVIEW32 software (Roper Scientific, Trenton, NJ). The camera features a 50 mm Cosmicar (Pentax) television lens with a minimum f# of 1.4. This lens is used in conjunction with a 20 mm extension tube to reduce the focal length of the lens to a more manageable length, resulting in a field of view that is 1.6×2.0 cm^2. A 620 nm cut-on filter is attached to the front of the lens to ensure only photons resulting from phosphorescent emission of the PrSBeads reach the CCD. The CCD is placed directly above the top window of the square syringe for optimal imaging of the PrSBeads being illuminated by the horizontal laser sheet. Synchronization between the pulsed excitation of the laser and the camera is achieved using a BNC-565 series pulse generator (Berkeley Nucleonics Corp., San Rafael, CA).

The MicroMAX camera allows the user to acquire two images in rapid succession. The exposure time of the first image is set by the user through the input provided in the WINVIEW 32 software. A nonvariable gap of 200 ns exists between the end of the first image acquisition and the beginning of acquisition of the second frame. The exposure time of the second frame is determined by the frame rate of the camera, as the electronic shutter remains "open" until both images are readout. Using 4×4 binning, the readout time is 78 ms, far longer than the lifetime of luminophore used in the PrSBeads. Preliminary experiments demonstrated that an acquisition time of 20 μs for the first image would provide enough signal-to-noise over the widest range of pressures for this system.

In addition to this primary portion of the setup, an auxiliary component is included to monitor rapidly changing oxygen concentrations within the syringe and to determine when equilibrium has been reached. Here, a 5 mW, 405 nm laser diode is used to excite a sample of PSP that is attached to the inside of the bottom window of the square syringe. This laser was modified to have a temporally controllable duty cycle that allows for the selective excitation of the PSP. The emission of the PSP is detected by a second photodiode positioned beneath the syringe. The pulsing of the 405 nm laser diode and the subsequent data collection by this second diode is also controlled via the NI-DAQ and LABVIEW, prior to the acquisition of lifetime measurements.

PSP Test Sample. The PSP used in these experiments was obtained from Innovative Scientific Solutions, Inc. (ISSI) of Dayton, Ohio. Marketed as UniFIB 470, the platinum-based PSP came premixed with a proprietary polymer binder designed for easy application by airbrush to test surfaces. Several samples were made by airbrushing the PSP onto the surface of clear polyethylene strips to allow for visualization of the PSP through the back. The strips were cut to the desired size for testing within the square syringe. One of the strips was attached to the inside of the bottom window of the syringe, and was dedicated to the monitoring of the oxygen concentration within the syringe.

Calibration of UniFIB 470 took place in a lab-built survey apparatus[4,19] that measured variations in phosphorescent emission intensity as a function of pressure in a temperature controlled environment. A fit to the linear Kavandi equation [Eq. (4)] results in coefficients of $A=0.89$ and $B=0.17$. Using these parameters, it is possible to determine the pressure (or oxygen concentration) within the square syringe from the intensity of PSP emission.

$$I_o/I = A + B(P/P_o). \tag{4}$$

In addition to measuring emission intensity as a function of pressure, the survey apparatus offers the capability to measure emission intensity as a function of temperature while holding pressure constant. At 1 atm of pressure, the PSP showed a temperature response of −0.5%/°C between 0 and 50 °C.

PrSBeads. Polystyrene microspheres, 2.5 μm in diameter, were doped with platinum octaethylporphyrin (PtOEP) as described by the synthetic procedure presented in Ref. 20. The PrSBeads are stored as a suspension in ethanol and are aerosolized through the use of a medical nebulizer discussed in detail in Ref. 18. A sample of the PrSBeads was prepared for calibration in the survey apparatus by drop-casting approximately 100 μl of PrSBeads suspended in ethanol (10% w/v) onto the surface of an aluminum coupon and allowed to dry. Intensity-based calibration of the PrSBeads was also performed using the survey apparatus described previously. A fit to the linear Kavandi equation results in coefficients of $A=0.23$ and $B=0.81$. A survey of temperature response shows a dependency of −1.1%/°C.

III. RESULTS AND DISCUSSION

A. Lifetime measurements from ModRLD of airborne PrSBeads

Lifetime measurements of airborne PrSBeads were made using the modRLD technique. Initially using the square syringe as a chamber to trap airborne PrSBeads in gases of varying oxygen concentrations, titration curves were produced to validate the ability of the technique to accurately determine the lifetimes. First, the empty chamber was filled with a gas mixture of the desired oxygen concentration counterbalanced with nitrogen. Then, the Nd:YAG laser was fired 25 times and 25 pairs of "blank" images were obtained. PrSBeads were then streamed into the syringe chamber at a rate of 2 l/min, carried in a gas of the desired oxygen concentration. Once an equilibrium of the oxygen concentration within the syringe was established, the laser was again fired 25 times and 25 frame pairs were acquired by the DIF-CCD as the PrSBeads flowed in ("flowing" condition). The syringe was then sealed, and 300 more frame pairs were acquired of the PrSBeads under no-flow conditions ("suspended" condition). The primary difference between these conditions is particle density within the syringe. When the PrSBeads are flowing into the syringe chamber, more particles are in the field of view, thus providing improved signal-to-noise. However, a continual flow of PrSBeads cannot be maintained in an experiment were the pressure within the syringe is changed by the movement of the syringe plunger. Therefore, it was necessary to ensure that a high enough particle density could be achieved and sustained under no-flow conditions.

Image processing began with the averaging of the 25 blank frame pairs to produce average blank, or background, images for both frames 1 and 2. These average background frames were then subtracted from the respective frames of flowing and settling PrSBeads. The average PrSBead intensities for these frames were calculated by first thresholding the image to create a binary mask, and using this mask to calculate an average intensity of the remaining pixels.

TABLE I. Calculated lifetimes for flowing and settling airborne PrSBeads.

P/P_o	$\tau_{fl} \pm 95\%$ CI (μs)	$\Delta P_{fl} \times 10^{-2}$ (atm)	$\tau_{su} \pm 95\%$ CI (μs)	$\Delta P_{fl} \times 10^{-2}$ (atm)
1	18.23 ± 0.06	3.26	18.85 ± 0.09	5.25
0.8	20.22 ± 0.02	0.36	20.37 ± 0.03	0.58
0.5	25.41 ± 0.03	0.21	25.35 ± 0.03	0.25
0.2	38.82 ± 0.03	0.06	38.91 ± 0.04	0.09
0	86.91 ± 0.07	0.02	86.93 ± 0.05	0.02

The average pixel intensity for each frame was used to calculate lifetimes via the modRLD technique. Particle motion from frame to frame was considered negligible, as frame pairs are separated in time by 200 ns. In extremely fast flows, one would expect the PrSBeads to appear as streaks, especially in frame 2, when the true exposure time is 76 ms. However, the phosphorescent lifetime of the PrSBeads is sufficiently short and the flow velocity is low enough to prevent particle streaking from occurring. Consequently, it was sufficient to take the average intensities from frame 1 and frame 2 and incorporate them into Eq. (2) to calculate lifetimes.

Lifetimes were calculated for all 25 frames of the PrSBeads flowing (τ_{fl}) into the syringe in various oxygen concentrations, and for 25 frames of the PrSBeads suspended (τ_{su}) in the square syringe. These values, along with 95% confidence intervals (CIs), are presented in Table I. As mentioned previously, measurements of PrSBeads flowing into the chamber have the benefit of higher particle densities and thus better signal-to-noise. This is reflected in smaller 95% CI and pressure error values. Kavandi plots of airborne PrSBeads flowing and settling within the square syringe are shown in Fig. 4. As a point of comparison, the Kavandi plot of stationary PrSBeads imaged by the DIF-CCD is also presented. Good agreement is shown between the sets of data.

However, as expected, 95% CI and pressure error values greatly increase when spatial averaging is reduced. For example, the 2×2 binning of pixels, while decreasing spatial resolution to half that of the full resolution offered by the CCD, also increases error values significantly. Pressure fluctuations in turbulent wake flows with $\mathrm{Re}=1.7\times10^5$, for example, can be shown to span about 0.036atm. Therefore, the large pressure uncertainties exhibited are unacceptable. It was found that the use of 8×8 pixel binning provided spa-

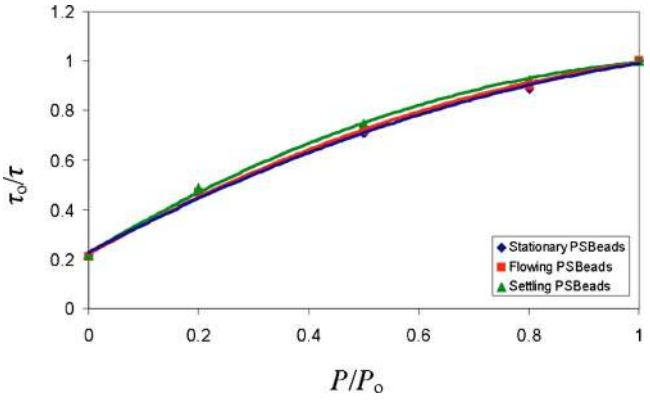

FIG. 4. (Color online) Kavandi plots of stationary PrSBeads within the square syringe for three separate runs.

TABLE II. Pressure resolutions (ΔP) for airborne PrSBeads at varying oxygen concentrations and interrogation window sizes.

	δ_P (atm)			
% O_2	2×2 pixels	8×8 pixels	16×16 pixels	32×32 pixels
21	0.465	0.109	0.052	0.027
16.8	0.273	0.058	0.029	0.017
10.5	0.130	0.029	0.015	0.009
4.2	0.056	0.014	0.007	0.004
0	0.021	0.005	0.003	0.002

tial resolution similar in size to the interrogation windows typically used in PIV while improving pressure data resolution to acceptable levels. Table II demonstrates how, as expected, increasing the size of the "interrogation" windows used, while decreasing the spatial resolution, improves the resolution of the pressure data.

B. Simultaneous pressure and velocity measurements from airborne PrSBeads

Stationary Experiments. A stationary PrSBeads slide was prepared by pipeting 100 μl of 2.5 μm diameter PrSBeads onto a glass slide and allowed to dry. The glass slide was then mounted within the square syringe at a 45° angle to allow for an orthogonal excitation/detection scheme. The pulsed Nd:YAG laser was used to excite the stationary PrSBeads, and the MicroMAX DIF-CCD fitted with a 620 nm cut-on filter was used to detect phosphorescence decay. Image acquisition was triggered approximately 1 μs after the laser pulse.

To maximize the pressure range of the system, each experiment was done in two parts. First, "low pressure" measurements ($P<1$ atm) were made by beginning with the plunger positioned all the way into the syringe and equalizing the pressure within the remaining volume (62.53 ml). The syringe was then sealed, and the plunger was pulled out using the syringe pump. The experiment would generally continue until a volume of ~80 ml was achieved. The pressure within the syringe was continually measured using the Omega absolute pressure transducer. The pressure drop over the course of the run was on the order of 22%. "High pressure" ($P>1$ atm) experiments would then be performed by equalizing the pressure within the syringe at its maximum volume, then closing all valves and pushing the plunger in with the syringe pump. Maximum pressures of 1.27 atm could be achieved.

A total of 225 laser pulses were delivered for each experiment at a rate of 6.4 Hz, resulting in 450 total images. The first 50 pulses were delivered with the plunger being held in its starting position. Then the plunger was moved and the pressure within the syringe was varied over the course of the final 175 pulses.

Recalling that PrSBeads have improved signal-to-noise and sensitivity at lower oxygen concentrations, the syringe was filled with a 10.5% oxygen mixture and the process was repeated. Using the same reference lifetime value as that in the 21% oxygen experiments and scaling the pressure, a combined Kavandi plot of the stationary PrSBeads in the two different environments was produced (Fig. 5). As a point of comparison, the binomial calibration curve of stationary PrSBeads in varying oxygen concentrations is also presented. Good agreement is shown among the sets of data, suggesting that an increase in sensitivity of PrSBeads at lower oxygen concentrations can indeed be expected.

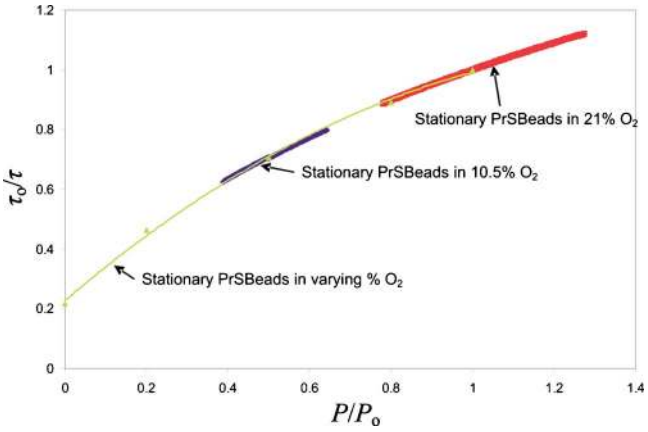

FIG. 5. (Color online) Combined Kavandi plot of stationary PrSBeads in the square syringe subjected to varying pressures in 10.5% and 21% O_2.

Airborne Studies. Once a reasonable expectation of the system's response was established, experiments involving airborne PrSBeads were performed. Using the setup described previously, airborne PrSBeads were aerosolized using a nebulizer driven by a carrier gas of 10.5% O_2 and passed over a bed of molecular sieves before entering the square syringe. After an equilibrium of the oxygen concentration within the syringe was established, all valves to the syringe were closed and data acquisition begun. A concentration of 10.5% O_2 was chosen for this experiment as it was expected to yield lifetime image pairs that were similar in intensity. In addition, the increased signal-to-noise and sensitivity gained by working in this environment was deemed necessary to resolve the expected pressure differences over the range of the syringe.

The airborne PrSBeads suspended within the syringe chamber were excited by the pulsed Nd:YAG laser. The laser beam was spread into a sheet that covered a 1.4×2 cm^2 area. The MicroMAX DIF-CCD was placed directly above the top window of the syringe, normal to the incoming laser sheet. The magnification of the camera was increased with a 20 mm extension tube so the field of view matched the area of excitation. A 620 nm cut-on filter was fitted to the front of the lens to isolate the phosphorescent emission of the PrSBeads. Image pairs were acquired by the camera at a rate of 6.4 Hz, approximately 1 μs after the pulsed excitation.

Each experiment consisted of 325 laser pulses for a total of 650 images. The first 150 pulses served as an equilibration period where the convection of the PrSBeads was monitored. After 150 pulses, the plunger of the syringe was moved (either in or out), and the motion and phosphorescence of the PrSBeads was followed over the final 175 pulses.

Figures 6 and 7 (left) display a frame sequence of airborne PrSBead phosphorescence as the plunger is moved out, thus lowering the pressure within the chamber. Plunger motion is from right to left. Figures 8 and 9 (left) display a

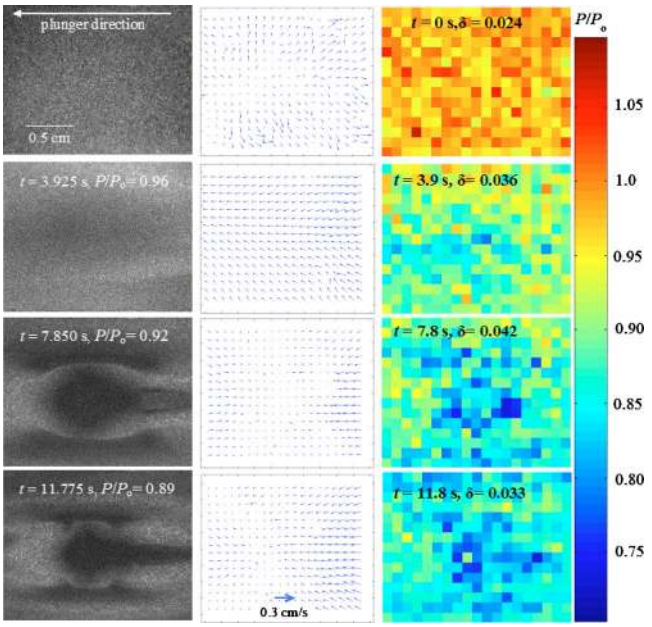

FIG. 6. (Color online) Raw images of airborne PrSBeads as the plunger is pulled out from right to left, from $t=0-11.775$ s (left). These velocity pairs were used to calculate velocity distributions over the field, shown in the center. Calculated pressure fields from airborne PrSBeads are shown on the right.

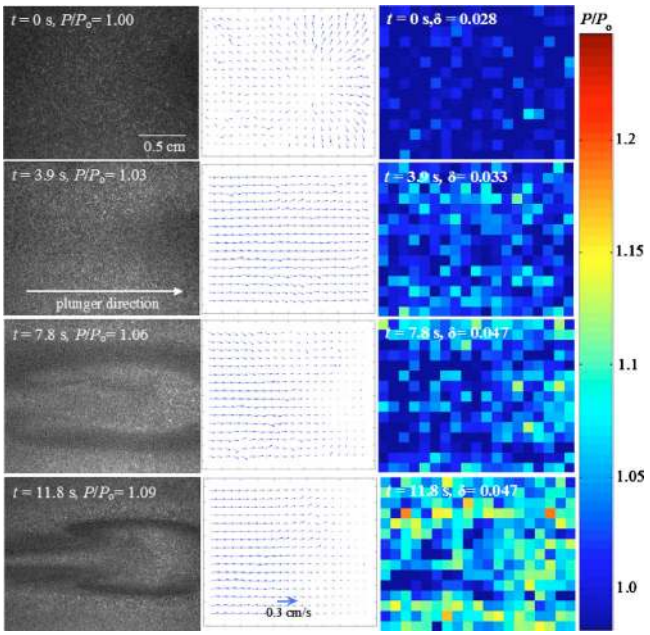

FIG. 8. (Color online) Raw images of airborne PrSBeads as the plunger is pushed in from right to left, from $t=0-11.8$ (left). These velocity pairs were used to calculate velocity distributions over the field, shown in the center. Calculated pressure fields from airborne PrSBeads are shown on the right.

frame sequence of airborne PrSBeads as the plunger is pushed in, moving from right to left. Accompanying each frame in both figures is a time stamp and P/P_o value as measured by the pressure transducer. In both sequences, the PrSBeads form axially symmetric, highly reproducible patterns across the field of view. These patterns are seen due to the variations in particle density that evolve over time. An estimation of the Reynolds number, $\mathrm{Re}=(\rho_\infty V_\infty d)/\mu_\infty$, of the flow within the syringe yields a value of ~ 2. In addition, visualization of the frame sequence as a movie reveals that much of the PrSBead motion appears to be in the z-direction, that is, into and out of the plane of the laser sheet, suggesting that convection cell patterns may be forming in the chamber. The immediate consequence of these patterns is the formation of "dark" regions within the field of view which form as

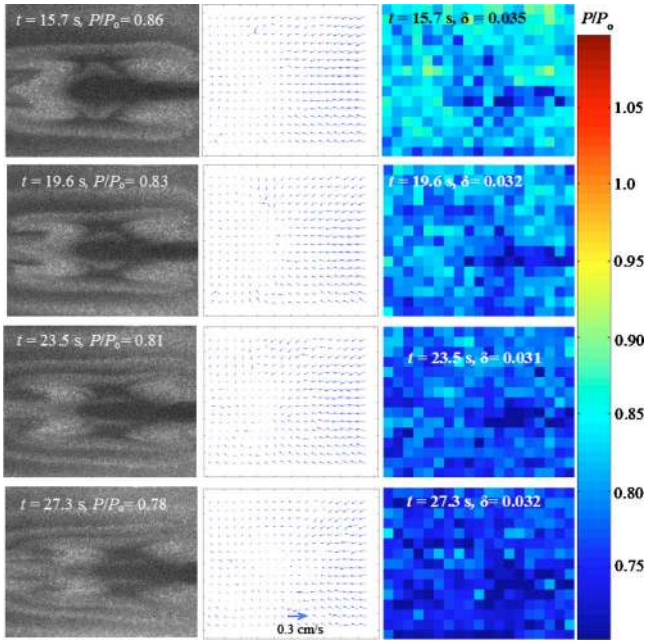

FIG. 7. (Color online) Raw images of airborne PrSBeads as the plunger is pulled out from right to left, from $t=15.7-27.3$ s (left). These velocity pairs were used to calculate velocity distributions over the field, shown in the center. Calculated pressure fields from airborne PrSBeads are shown on the right.

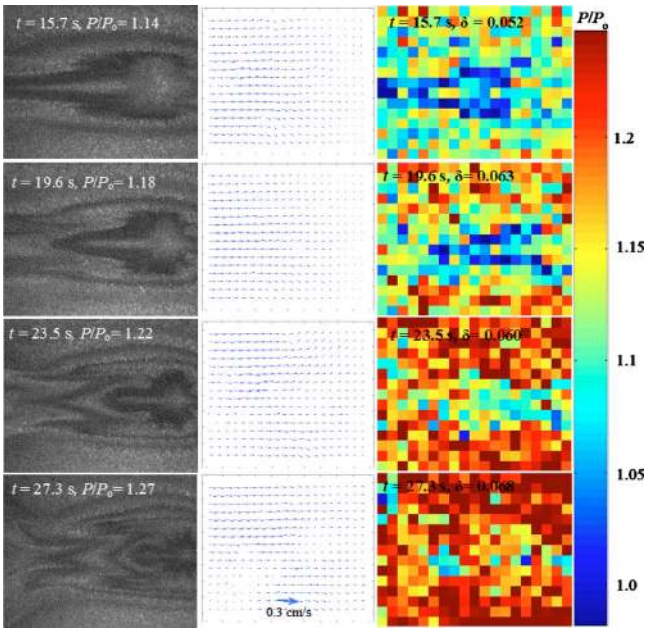

FIG. 9. (Color online) Raw images of airborne PrSBeads as the plunger is pushed in from right to left, from $t=15.7-27.3$ s (left). These velocity pairs were used to calculate velocity distribution over the field, shown in the center. Calculated pressure fields from airborne PrSBeads are shown on the right.

TABLE III. Pressure transducer and airborne PrSBeads P/P_o ratios for the frame pairs in Figs. 6 and 7.

Time (s)	Transducer (P/P_o)	PrSBeads (P/P_o)	δ
0	0.999	0.979	0.024
3.92	0.964	0.901	0.036
7.84	0.927	0.866	0.042
11.76	0.893	0.849	0.033
15.69	0.862	0.821	0.035
19.61	0.833	0.794	0.032
23.53	0.806	0.770	0.031
27.29	0.783	0.747	0.032

the result of convective mining of regions of lower density, such as regions near the walls. The particle density in these regions may be significantly reduced to the point where there is insufficient signal-to-noise to provide accurate lifetime data. In addition, regions lacking particles will also negatively affect DPIV measurements across the field of view. To counter this effect, larger interrogation windows are necessary, thus reducing the spatial resolution of the data.

Therefore, lifetime calculations across the field of view were performed using 16×16 pixel interrogation windows. As the pressure gradients within the flow are within the noise of the system, uniform pressure distributions across the field are expected. Figures 6 and 7 (right) shows the two-dimensional pressure distributions within the square syringe that correspond to the frame sequence in Figs. 6 and 7 (left), respectively. As expected, a global pressure drop is exhibited from start to finish that corresponds to the data presented in Fig. 4. Figures 8 and 9 (right) displays the pressure distributions for the frame sequence in Figs. 8 and 9 (left), respectively. A pressure increase is seen that also correlates to the data presented in Fig. 6. In all cases, a bias toward lower pressure measurements is seen in regions of low particle density. It is believed that these regions of poor signal-to-noise are the major contributor to the δ values reported. In both Figs. 6 and 7 (right), the P/P_o fields at $t=0$ s, where particle density is still high and relatively uniform, deviations over the fields are between 30% and 47% less than the average deviations of the remaining frames. Tables III and IV summarize these results, including P/P_o ratios as measured by the absolute pressure transducer and calculated from airborne PrSBeads, and the standard deviation of the P/P_o measurements across the field of PrSBeads.

TABLE IV. Pressure transducer and airborne PrSBeads P/P_o ratios for the frame pairs in Figs. 8 and 9.

Time (s)	Transducer (P/P_o)	PrSBeads (P/P_o)	δ
0	1.000	0.9788	0.028
3.92	1.028	1.017	0.033
7.84	1.060	1.019	0.047
11.76	1.095	1.066	0.047
15.69	1.135	1.109	0.052
19.61	1.177	1.141	0.063
23.53	1.221	1.186	0.060
27.29	1.265	1.218	0.068

As is evident in these tables, there is a significant deviation between the P/P_o values measured by the pressure transducers and those calculated from lifetime measurements of airborne PrSBeads. With respect to time, these are the first measurements of each experiment, as the plunger is first moved in or out of the syringe. Interestingly, the deviation appears to be continuous through the two different experimental conditions.

Simultaneous Pressure and Velocity Measurements. Digital particle imaging velocimetry was then performed using the phosphorescence images of the airborne PrSBeads to demonstrate the ability to simultaneously measure pressure and velocity within a gas phase flow. Traditional PIV computes the cross-correlation (yielding displacement) between patterns of particles between two images separated by a finite and known duration of time, Δt. In the present experimental setup, Δt was limited to 0.157 s (corresponding to the camera's 6.4 Hz frame rate), which was the readout rate of the DIF-CCD. Flow velocities within the square syringe were expected to be on the order of 0.15 cm/s, which is the maximum speed of the plunger being moved by the syringe pump. At that maximum velocity, PrSBeads can be expected to be displaced 2.3×10^{-4} cm. Considering the field of view was 1.4×2.0 cm^2, a 2.3×10^{-4} cm shift equates to linear movement of 3.7 pixels, and can be contained within a 16×16 pixel interrogation window.

It is important to note that the temporal resolution of the pressure data collected in this experiment is twice that of the velocity data, since two laser pulses are needed to produce images appropriately spaced in time. Pressures are calculated with each laser pulse from the pair of images collected by the DIF-CCD that detect the phosphorescent decay of the PrSBeads. To that end, in the following discussion, the term "pressure pairs" refer to the two images collected from a single laser pulse, whereas "velocity pairs" are two images collected from consecutive laser pulses.

PIV calculations were performed using MATPIV 1.6.1 (Refs. 21 and 22) run on the MATLAB platform. To provide a distance calibration reference, a grid with 0.5 cm divisions was placed within the square syringe covering the region of interest. The image was then used to specify the coordinate system for the MATPIV software. Once points of the grid are manually chosen and defined, a linear mapping function correlates the pixel sizes to actual distances. Velocity pair images could then be processed by the MATPIV algorithm with user defined parameters. For these images, six passes of the data were made, starting with interrogation windows 64×64 pixels in size and ending with 16×16 pixel windows. To match the spatial resolution of the pressure data, no window overlap was used. The data were then filtered using the default parameters to remove spurious vectors in the velocity field and finally missing vectors were replaced using nearest neighbor interpolation. Figures 6–9 (center) show the resulting velocity fields corresponding to the pressure distributions shown in Figs. 6–9 (right), respectively. The vectors in the velocity fields have been scaled for improved visualization of the relative magnitudes and directions. A scale bar representing the magnitude of a 0.3 cm/s vector is shown in the bottom right frame of each figure.

IV. CONCLUSION AND FUTURE WORK

Quantitative pressure measurements of airborne PrSBeads in gaseous flows have been performed through the modRLD method. A titration of airborne PrSBeads in carrier gases containing varying concentrations of oxygen displayed good agreement with measurements made using stationary PrSBeads. Error analysis demonstrated that 25 pulse averages can provide pressure measurements with a precision between 0.1 and 1% of 1 atm.

Pressure measurements over the entire field of view of the DIF-CCD were made by employing the use of interrogation windows, where the phosphorescence of the PrSBeads over a binned number of pixels was averaged and used to calculate lifetimes. It was shown that the precision in pressure measurements made over the entire field of view for single pulses is highly dependent upon the size of the interrogation windows used. Two-by-two pixel windows resulted in standard deviations of pressure measurements on the order of 0.5 atm at 1 atm. The use of 32×32 pixel windows reduced the deviations to 0.009 atm at 0.5 atm of pressure. While the use of signal averaging would improve the precision of the measurements, such averaging may not be possible when studying turbulent flow phenomena.

Pressure measurements in the air within a square syringe as its plunger was moved in and out were also made using airborne PrSBeads. The use of 16×16 pixel interrogation windows provided instantaneous pressure measurements over the field of view with a precision of 3%–5%. It was found that the fluid motion within the square syringe cause cells of PrSBeads to form, resulting in pockets of low PrSBead density. The regions are the primary sources of error, as insufficient signal-to-noise of PrSBead phosphorescence could be obtained. However, the global pressure change in the air within the square syringe was clearly evident as the pressure ranged between 0.78 and 1.3 atm.

At present, the technique is limited by hardware to low signal-to-noise, and slow CCD readout. We are present pursuing resolving these issues by obtaining CCDs with a faster readout as well as deeper well capacities. Also, it has been shown that the PrSBeads behave as a nonideal PSP with respect to their temperature sensitivity. Temperature coefficients for the PrSBeads can range between -0.23 and -0.48 $\mu s/°C$ over an 1 atm pressure range. Therefore, an adequate temperature correction scheme will need to be utilized to correct for temperature effects within turbulent flows. A solution that is currently being investigated is the implementation of a dual-luminophor, pressure and temperature sensitive microsphere that borrows upon dual-luminophor PSP technology.[23] Known as TPrSBeads, it is hoped that these microspheres can provide simultaneous temperature, pressure, and velocimetry data of gaseous flows. The temperature data could then be used to correct for the temperature sensitivity of the pressure measurements, thus improving its accuracy.

ACKNOWLEDGMENTS

This work is supported by the National Science Foundation (Grant No. 0517782), Air Force Office of Scientific Research (Grant No. STTR AF04-T001), Innovative Scientific Solutions Inc., and the University of Washington Royalty Research Fund (Grant No. 65-1295). We would also like to thank Roy Olund and John Heutink of the Electronic and Machine Shops of the Chemistry Department for their assistance with the experimental aspects of this research.

[1] M. Gouterman, J. Chem. Educ. **74**, 697 (1997).
[2] J. R. Lakowicz, *Principles of Fluorescence Spectroscopy* (Plenum, New York, 1983), p. 1.
[3] L. Coyle, "Lifetime Measurements on Pressure Sensitive Paints: Temperature Correction, Effects of Environment, and Trials on New Luminescent Materials," Thesis, University of Washington, 1999.
[4] J. H. Bell, E. T. Schairer, L. A. Hand, and R. D. Mehta, Annu. Rev. Fluid Mech. **33**, 155 (2001).
[5] A. Baron, "On Time and Spatially Resolved Measurements of Luminescence-Based Oxygen Sensors," Thesis, University of Washington, 1996.
[6] G. Dale, A. Baron, C. Tyler, and V. Mastrocola, Proceedings of the International Congress Instrumentation in Aerospace Simulation Facilities 1997 (ICIASF '97), 1997, pp. 40–45.
[7] S. P. Chan, Z. J. Fuller, J. N. Demas, and B. A. DeGraff, Anal. Chem. **73**, 4486 (2001).
[8] J. N. Demas, *Excited State Lifetime Measurements* (Academic, New York, 1983).
[9] J. H. Waite, Anal. Chem. **56**, 1935 (1984).
[10] C. Moore, S. P. Chan, J. N. Demas, and B. A. DeGraff, Appl. Spectrosc. **58**, 603 (2004).
[11] T. Q. Ni and L. A. Melton, Appl. Spectrosc. **47**, 773 (1993); **50**, 1112 (1996).
[12] Terminology used by Princeton Instruments MicroMAX camera.
[13] C. McGraw, Thesis, University of Washington, 2004.
[14] H. Hu and M. M. Koochesfahani, Exp. Fluids **33**, 202 (2002).
[15] M. Gharib and D. Dabiri, in *Flow Visualization*, edited by A. J. Smits and T. T. Lim (World Scientific, Singapore, 2000), pp. 123–147.
[16] C. E. Willert and M. Gharib, Exp. Fluids **10**, 181 (1991).
[17] S. Abe, K. Okamoto, and H. Madarame, Meas. Sci. Technol. **15**, 1153 (2004).
[18] S. Zumdahl, *Chemical Principles*, 5th ed. (Houghton Mifflin, Boston, 2005), pp. 141–143.
[19] S. Danielson, *Instrumentation Manual for Phosphorescent Emission Intensity Measurements* (Internal Publication, University of Washington, 1990).
[20] S. H. Im, G. Khalil, J. Callis, B. H. Ahn, and Y. Xia, Talanta **67**, 492 (2005).
[21] This program is offered as freeware from http://www.math.uio.no/~jks/matpiv/.
[22] J. K. Sveen and E. A. Cowen, in *PIV and Water Waves*, edited by J. Grue, P. L. F. Liu, and G. K. Pederson (World Scientific, Singapore, 2004), pp. 1–49.
[23] B. Zelelow, G. E. Khalil, G. Phelan, B. Carlson, M. Gouterman, J. B. Callis, and L. R. Dalton, Sens. Actuators B **96**, 304 (2003).